ORIGINAL RESEARCH

Chlorambucil-Iron Oxide Nanoparticles as a Drug Delivery System for Leukemia Cancer Cells

Samer Hasan Hussein-Al-Ali [1,2]
Mohd Zobir Hussein [3]
Saifullah Bullo[3]
Palanisamy Arulselvan [4]

[1]Faculty of Pharmacy, Isra University, Amman, 11622, Jordan; [2]Department of Chemistry, Faculty of Science, Isra University, Amman, 11622, Jordan; [3]Materials Synthesis and Characterization Laboratory, Institute of Advanced Technology (ITMA), Universiti Putra Malaysia, Selangor, 43400, Malaysia; [4]Laboratory of Vaccines and Immunotherapeutic, Institute of Bioscience, Universiti Putra Malyasia, Serdange, Selangor, 43400 UPM, Malaysia

Introduction: Traditional cancer therapies may have incomplete eradication of cancer or destroy the normal cells. Nanotechnology solves the demerit by a guide in surgical resection of tumors, targeted chemotherapies, selective to cancerous cells, etc. This new technology can reduce the risk to the patient and automatically increased the probability of survival. Toward this goal, novel iron oxide nanoparticles (IONPs) coupled with leukemia anti-cancer drug were prepared and assessed.

Methods: The IONPs were prepared by the co-precipitation method using Fe^{+3}/Fe^{+2} ratio of 2:1. These IONPs were used as a carrier for chlorambucil (Chloramb), where the IONPs serve as the cores and chitosan (CS) as a polymeric shell to form Chloramb-CS-IONPs. The products were characterized using transmission electron microscopy (TEM), powder X-ray diffraction (PXRD), scanning electron microscopy (SEM) analysis, Fourier transform infra-red spectroscopy (FTIR), vibrating sample magnetometry (VSM) analyses, and thermal gravimetric analysis (TGA).

Results: The as-prepared IONPs were found to be magnetite (Fe_3O_4) and were coated by the CS polymer/Chloramb drug for the formation of the Chloramb-CS-IONPs. The average size for CS-IONPs and Chloramb-CS-IONPs nanocomposite was found to be 15 nm, with a drug loading of 19% for the letter. The release of the drug from the nanocomposite was found to be of a controlled-release manner with around 89.9% of the drug was released within about 5000 min and governed by the pseudo-second order. The in vitro cytotoxicity studies of CS-IONPs and Chloramb-CS-IONPs nanocomposite were tested on the normal fibroblast cell lines (3T3) and leukemia cancer cell lines (WEHI). Chloramb in Chloramb-CS-IONPs nanocomposite was found to be more efficient compared to its free form.

Conclusion: This work shows that Chloramb-CS-IONPs nanocomposite is a promising candidate for magnetically targeted drug delivery for leukemia anti-cancer agents.

Keywords: chlorambucil, anticancer, leukemia cell lines, magnetic nanoparticles, sustained release

Correspondence: Mohd Zobir Hussein
Materials Synthesis and Characterization Laboratory, Institute of Advanced Technology (ITMA), Malaysia Universiti Putra Malaysia, UPM, Serdang, Selangor, 43400, Malaysia
Tel +603 89466801
Fax +603 89435380
Email mzobir@upm.edu.my

Samer Hasan Hussein-Al-Ali
Department of Chemistry, Faculty of Science, Isra University, P.O. Box 22, Amman, 11622, Jordan
Tel +962 4711710
Fax +962 4711505
Email samer.alali@iu.edu.jo

Introduction

Leukemia is one of the hematologic malignancies diseases which is most common in adults which affects the bone marrow, lymphatic system and blood cells.[1] Leukemia is clonal hematopoiesis created in the bone marrow and is discovered by the uncontrollable generation of poorly differentiated white blood cells. Treatment of this disease depends on several factors; type of leukemia, age, the extent of the disease and patient history. The treatment regimes for the patients are usually targeted therapy (chemotherapy), radiation therapy and bone marrow transplantation.[2]

6205

Based on the degree of cell generation (chronic or acute) and type of cell affected (lymphoid or myeloid), the leukemia disease can be classified into four main categories; chronic myeloid leukemia (CML), acute lymphocytic leukemia (ALL), chronic lymphocytic leukemia (CLL) and acute myeloid leukemia (AML). AML leukemia is the most common type in adults and ALL is more prevalent among pediatric patients.[1] The difference between CML and CLL depends on the white blood cells that have become cancer cells. In CLL, the abnormal cells develop from lymphoid blood stem cells (B cells), while the CML developed from myeloid blood stem cells.[3,4]

Traditional cancer therapies such as surgery, chemotherapy and radiation methods may have incomplete eradication of cancer or destroy the normal cells. Nanotechnology solves the demerit of these traditional methods by a guide in surgical resection of tumors, target chemotherapies directly, and selective to cancerous cells.[5] This new technology can reduce the risk to the patient and automatically increased the probability of survival.

Toward this goal, polymers nanoparticles with particle size less than 200 nm were prepared and anticancer drugs were dissolved, encapsulated, adsorbed or entrapped into them.[6,7] Using this approach, different anticancer drugs were delivered to cancer cells, such as tamoxifen,[8] docetaxel,[9] psoralen,[10] erlotinib/ doxorubicin,[11] ciprofloxacin[12] and betulinic acid.[13]

IONPs have been used to enhance the therapeutic act of anticancer drugs and decrease the side effects that are usually attached to the conventional treatment of cancer. IONPs loaded with different drugs, such as doxorubicin,[14–16] paclitaxel,[17–19] cisplatin,[20,21] gemcitabine,[22] methotrexate,[23] and docetaxel[24] have been successfully prepared and used for cancer treatment.

Dou's group has studied the effect of cytosine arabinoside-magnetic nanoparticles on leukemia stem cells (LSCs). The results showed that cytosine arabinoside-magnetic nanoparticles have a significant increase in apoptosis and reactive oxygen species (ROS) levels compared to cytosine arabinoside. This result indicates that the prepared nanocomposites can improve the expression of pro-oxidation molecule gp91-phox and decreased the expression of antioxidant molecule superoxide dismutase-1.[25] Ferumoxytol that is composed of superparamagnetic iron oxide, coated with a carbohydrate shell has been approved by the US Food and Drug Administration (FDA) to be used for iron deficiency treatment. Trujillo-Alonso et al have shown that low expression of the iron exporter ferroportin membrane

resulted in susceptibility of leukemia cell lines via an increase in intracellular iron from ferumoxytol. The reactive oxygen species produced by free Fe^{+2} iron lead to increased oxidative stress and cell death.[26]

The target in pharmaceutical science is to transport the maximum rate of the drug across a biological membrane. Therefore, solubility plays an important role in drug absorption, distribution, metabolism and excretion. The use of several poorly water-soluble drugs, such as chlorambucil has late risen sharply. Development of new formulations of the poorly soluble drug can put forward the significant challenges at all stages of drug development. The low bioavailability of these drugs may lead to delays in biological activities.[27]

Different techniques were used for the enhancement of the solubility of the poorly water-soluble drug and to improve its bioavailability. These include; particle size reduction, nanosuspension technology, surfactant, salt formation, pH adjustment, hydrotrophy and solid dispersion.[28]

Chlorambucil has a Leukeran common name and the IUPAC name is 4-[4-[bis (2-chloroethyl)amino]phenyl] butanoic acid. It is a bifunctional alkylating compound, medically used for the therapeutics of CLL and CML leukemia, lymphomas. The toxicity of Chloramb was due to the alkylating part; therefore, toxicity attitude on its oxidative stress-inducing behavior that applies equally against normal and cancer tissues.[29,30]

Different polymers were used to enhance the chlorambucil activity, which include poly (butyl cyanoacrylate),[31] linear-globular PEG,[32] hydroxychloroquine,[33] and poly (lactide-co-glycolide).[34] Chlorambucil-loaded poly (butyl cyanoacrylate) preparations have been shown to increase drug stability, thus avoiding drug hydrolysis.[31] In addition, Chlorambucil conjugated with anionic linear-globular dendrimer has decreased the insolubility of Chlorambucil in water and improved the anticancer activity in vitro and in vivo.[32] Capolla research group has shown that monoclonal antibodies (anti-CD20) nanoparticles containing hydroxychloroquine (HCQ) and Chlorambucil (CLB) (HCQ+CLB) can be effective as a single therapeutic agent in controlling aggressive leukemia.[33] Another research aims to improve the activity of Chlorambucil through using poly (DL-lactide-co-glycolide) (PLGA) have shown PLGA-Chlorambucil has higher activity on the non-Hodgkin's lymphoma compared to the free drug.[34]

Our work aimed to produce and characterize a new drug-IONPs. We produced Chloramb-CS-IONPs nanocomposite where IONP is as the core of the nanocomposite and the CS

polymer is as the shell. The nanocomposites were investigated for their cytotoxicity on normal fibroblast and leukemia cancer cell lines. To the best of our knowledge, this is the first new Chloramb-CS-IONPs nanocomposite that was prepared, where its therapeutic effects of targeted nanocomposite at leukemia cell lines were studied.

Materials and Methods
Materials
Chlorambucil, iron (III) chloride (>99%), iron (II) chloride (>99%) were obtained from Merck KGaA (Darmstadt, Germany). Chitosan (L.M.W) with 75–85% deacetylation degree was purchased from Sigma-Aldrich (Saint Louis, MO, USA). The Dulbecco's modified Eagle's medium (DMEM), and MTT kit (3-(4,5-dimethylthiazol-2-yl)-2,5-diphenyltetrazolium bromide) were purchased from Sigma-Aldrich (Saint Louis, MO, USA). NIH 3T3 cell lines murine and cancer WEHI cell lines were purchased from the American Type Culture Collection (ATCC, Manassas, VA).

Preparation of IONPs
Preparation of IONPs with the formula, Fe_3O_4 was carried out using the co-precipitation method.[35,36] A molar ratio of 2:1 of Fe (III) (0.3 M) to Fe (II) (0.15 M) was added to a solution of 2 M NaOH drop-wise with stirring at 25°C and the pH value was kept above 10. The resulting IONPs were then sonicated for 15 minutes, collected by ultracentrifugal separation. The excess of NaOH was removed by washing four times with deionized water. The IONPs were then kept in an oven at 45°C for 6 hours.

Preparation of CS-IONPs Nanoparticles
The preparation of CS-IONPs nanoparticles was adopted as previously described in the literature.[35,36] Briefly, the CS solution was prepared by dissolving 2.0 g of CS into 1% acetic acid. The CS-IONPs nanoparticles were prepared by adding the CS solution into a 5 mg/mL suspension of IONPs. The resulted CS-IONPs were then stirred thoroughly for 18 hours at 25°C and separated by a permanent magnet.

Preparations of Chloramb-CS-IONPs Nanocomposite
The Chloramb-CS-IONPs nanocomposite was collected by mixing 50 mg of Chloramb with 200 mg of CS-IONPs. The resulting sample was stirred at room temperature for 18 hours to ease the uptake of Chlorambucil. The final nanocomposite was separated using a permanent magnet.

The Chloramb Loading Efficiency (%LE) in Nanocomposite
The loading efficiency of Chlorambucil into the nanocomposite was determined by separating the supernatant from the solid nanoparticles by ultracentrifugation at 15000 rpm for 30 min. The amount of unloaded Chloramb in the supernatant was measured by a UV spectrophotometer using Eq 1.,

$$\%LE = \frac{M_t - M_f}{\text{mass of nanocomposite}} \times 100 \qquad (1)$$

where Mt is the total Chloramb used in the experiment and Mf is the unloaded Chloramb.

The Release of Chloramb from Chloramb-CS-IONPs Nanocomposite
Chloramb release profile from the Chloramb-CS-IONPs nanocomposite was determined using a phosphate-buffered saline solution (PBS) at pH 7.4. About 300 mg of the Chloramb-CS-IONPs was added into a vessel containing 500 mL of the buffer solution. The released amount of Chloramb was determined at preset time intervals using a Shimadzu UV-1601 spectrophotometer.

3T3, WEHI Cells Culturing and MTT Cytotoxicity Assays
The 3T3 and WEHI cells were placed in Dulbecco's Modified Eagle medium in 5% CO_2 in a humidified incubator. Confluent cells were seeded into a 96-well plate at 1×10^5 cells/mL and kept overnight. A 100 μL from a new medium containing Chloramb, CS-IONPs and Chloramb-CS-IONPs were used to treat the cells. For each sample, fresh solutions of Chloramb, CS-IONPs and Chloramb-CS-IONPs were used for the treatment with concentrations starting from 3.125 μg mL^{-1} up to 100 μg mL^{-1}. The MTT assay was used 72 hours to study the toxic effect of Chloramb, CS-IONPs and Chloramb-CS-IONPs samples.

The experiment was performed in triplicate and absorption was measured at a wavelength of 570 nm, and the data of cell viability was expressed as the mean± SD as given in Eq 2.

$$\%\text{Cell Viability} = \frac{\text{Average of treated}}{\text{Average Control}} \times 100 \qquad (2)$$

Instrumentation
X-ray diffraction (XRD) technique was used to study the crystal structure of the Chloramb, CS-IONPs and Chloramb-

CS-IONPs in the range of 20–70° by XRD-6000 diffractometer with CuK$_\alpha$ radiation, λ=1.5406 Å, 30 kV and 30 mA (Shimadzu, Tokyo, Japan). Fourier transform infrared spectroscopy (FTIR) spectra of the Chloramb, CS-IONPs and Chloramb-CS-IONPs were recorded between 400 and 4000 cm^{-1} (Thermo Nicolet Nexus). Thermogravimetric analysis (TGA) was carried in the range of 30–900°C with a heating rate of 10 °C·min^{-1}, in 150 μL alumina crucibles (Metter-Toledo 851e instrument (Switzerland)). The particle size of the CS-IONPs and Chloramb-CS-IONPs were collected using a transmission electron microscope (TEM) (Hitachi H-7100, Tokyo, Japan). UV-Vis spectra were used to study the release behavior, using a Shimadzu UV-1601 spectrophotometer.

Result and Discussion
Powder XRD Patterns
The color of IONPs depends on their chemical composition. The jet-black color refers to magnetite (Fe_3O_4) or maghemite (γ-Fe_2O_3) structures whereas the brownish-red color indicates a mixture of IONPs (magnetite, maghemite and goethite).[37,38] Figure 1A–C shows the XRD patterns of IONPs, CS-IONPs and Chloramb-CS-IONPs, respectively. The six characteristic peaks for Figure 1A at 30.1°, 35.5°, 43.1°, 53.5°, 57.2° and 62.9°, which corresponding to the 220, 311, 400, 422, 511 and 440 planes, respectively, indicating the formation of iron oxide magnetite structure with jet-black color.[39] In addition, the absence of 210 and 300 reflections in the XRD pattern indicates that the maghemite is not present in the samples. Interestingly, the broadening of peaks of IONPs was nearly similar to that of CS-IONPs as shown in Figure 1B. The similar broadening of XRD peaks is predominantly attributed to the unchanging crystallite size. Figure 1C shows the XRD patterns of Chloramb-CS-IONPs nanocomposite, indicating that there is no Chloramb peaks are present in the nanocomposite. This result suggests that the Chloramb drug was probably incorporated inside of the nanocomposite instead of at the surfaces.

Fourier Transform Infrared Spectroscopy

Figure 2A–D shows the Fourier transformed infrared spectroscopy (FTIR) spectra of pure Chloramb, IONPs, CS-IONPs and Chloramb-CS-IONPs, respectively. The carboxylic acid group for Chloramb shows a strong and very wideband for the O–H stretching vibration in the
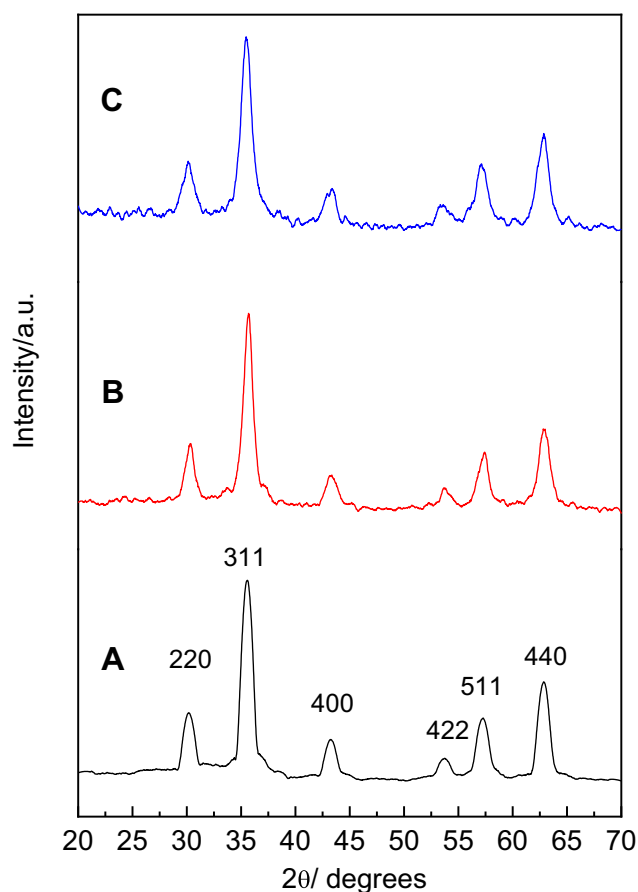

Figure 1 XRD patterns of IONPs (**A**), CS-IONPs (**B**), and Chloramb-CS-IONPs (**C**).

region 3300–2500 cm^{-1}, centered at about 2935 cm^{-1}. This is in the same region as the C–H stretching bands of both alkyl and aromatic groups. The carbonyl stretching band of the C=O of the carboxylic group for Chloramb appears as an intense band at 1701 cm^{-1}. The C–O stretching vibration for COOH appears in the region 1320–1210 cm^{-1}, centered at about 1232 cm^{-1}. The O–H bending appeared with a strong band at 1360 cm^{-1} and 946 cm^{-1}. The benzene ring for Chloramb shows absorptions at 1615 cm^{-1} and 1447 cm^{-1} due to the C=C stretching vibrational modes. A band in the region of 1250–1000 cm^{-1} is due to the C–H in-plane bending of the benzene ring. The aromatic amines (C-N) was appeared as a strong band at 1309 cm^{-1}, while the aliphatic amine vibrational band appears at 1180 cm^{-1}. The C-Cl bond gives two bands at 744 and 723 cm^{-1}.
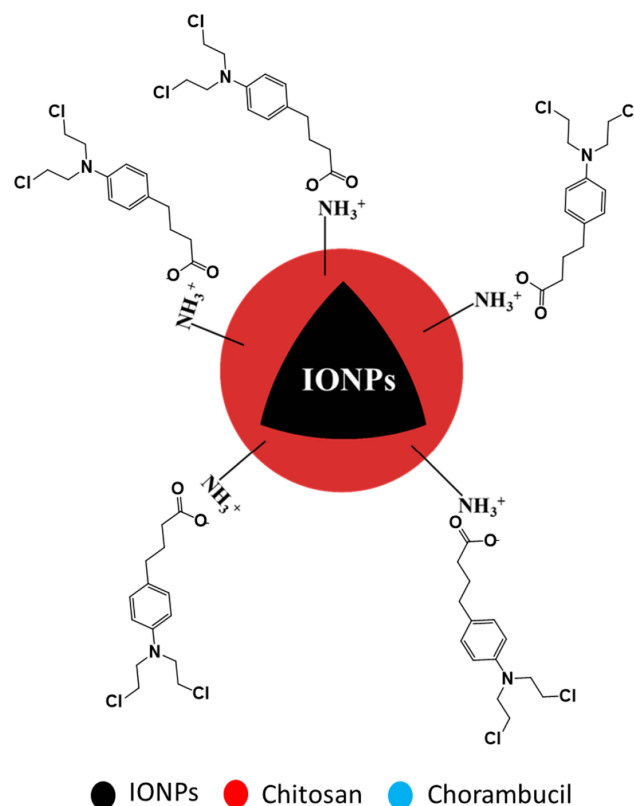
Figure 2B exhibits the FTIR spectrum of IONPs nanoparticles with various bands at 3411, 1626, 1562, 1338, 864 and 538 cm^{-1}. The peaks at 538 and 864 cm^{-1} are due to the presence of Fe-O, which indicates that the synthesized nanoparticles are iron oxide.[40] Furthermore, the two
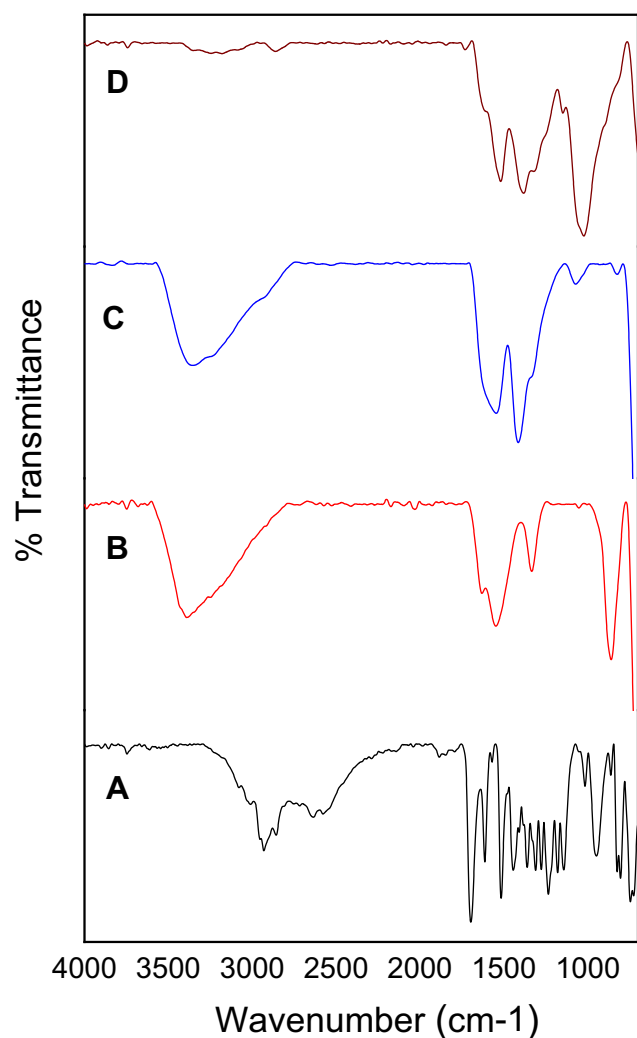
Figure 2 FTIR spectrum of Chloramb (**A**), IONPs (**B**), CS-IONPs (**C**), and Chloramb-CS-IONPs (**D**).

Figure 3 Molecular structure model of chloramb intercalated with IONPs.

bands at 1626 cm^{-1} and 3411 cm^{-1} can be attributed to the bending vibration of absorbed water and the surface hydroxyl group, respectively.[41]

In the case of CS-IONPs nanoparticles (Figure 2C), the CS is indicated by the presence of a small band at 2922 cm^{-1} due to the vibrational mode of –CH– in CS. A band at 1573 cm^{-1} is due to the vibrational mode of N–H in the CS. In addition, the C-N vibration of the amino group is at 1416 cm^{-1} and the C–O in the ether group is at 1069 cm^{-1}. The comparison of the FTIR spectra of Chloramb-CS-IONPs with that of CS-IONPs shows that the band at 1613 cm^{-1} is attributed to the C=C stretching vibration of the aromatic ring. In addition, the absence of a band at 1701 cm^{-1} that is for carbonyl in the carboxylic group and at the same time two new intense bands at 1613 and 1391 cm^{-1} are attributed to the asymmetric and

symmetric carboxylate stretching of the Chloramb anions, respectively. These indicate that the interaction between the protonated amine group of CS with the carboxylate group of Chloramb has taken place (Figure 3).

Thermal Gravimetric Analysis (TGA-DTG)

The Chloramb loaded on the IONPs and thermal properties were studied by thermogravimetric analysis (TGA). Figure 4A–D) show the thermal properties for Chloramb, IONPs, CS-IONPs and Chloramb-CS-IONPs, respectively. The decomposition stage of Chloramb in Figure 4A is starting at around 180°C. Nevertheless, there are two major steps for the weight loss of the Chloramb drug. The first weight loss started at around 180°C and ended at around 322°C with a total weight loss of 28%. The second weight loss starting at around 322°C and ended at around 525°C with 43% weight loss. These two major steps were due to the decomposition of the benzene ring and the side chain of Chloramb.

The thermal analysis of IONPs, and CS-IONPs are shown in Figure 4B and C), respectively. The TGA curve of IONPs represented weight loss of around 5.2%
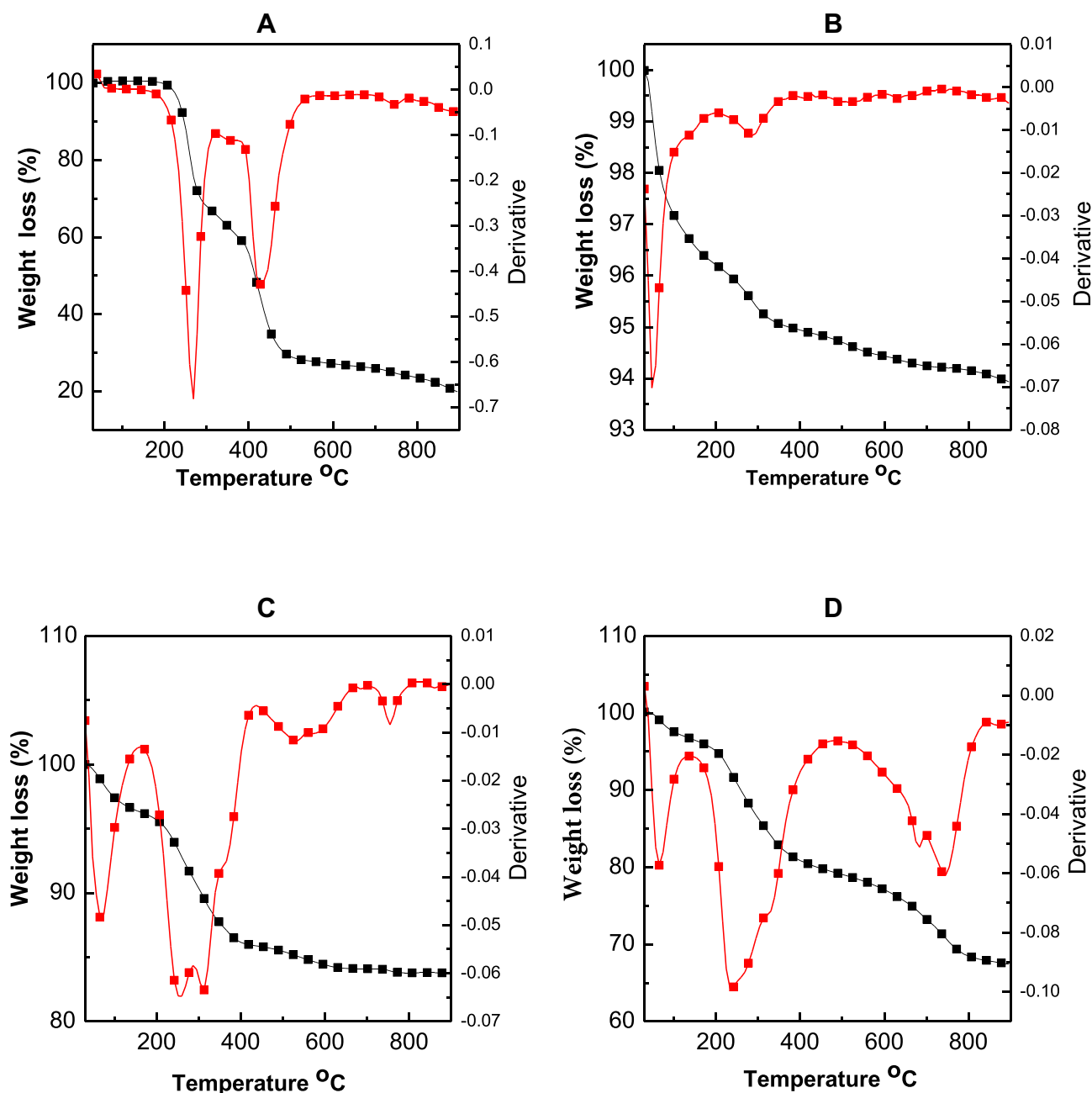
Figure 4 Thermal gravimetric analysis curves of Chloramb (**A**), IONPs (**B**), CS-IONPs (**C**) and Chloramb-CS-IONPs (**D**).

with two major steps at 48 and 286°C, respectively. These weight losses were due to the removal of surface hydroxyl groups (OH) and/or adsorbed water.

After CS-IONPs were prepared, the total weight loss of CS-IONPs increased higher than that of IONPs. This fact was due to the CS polymer-coated the IONPs. The total weight loss of CS-IONPs was 15.5%, while IONPs have a 5.2%.

For Chloramb-CS-IONPs, three stages of weight loss are observed in Figure 4D. The first weight loss step occurs between 30 and 136 °C with weight losses of 3.1%. The step of weight loss is attributed to the removal of surface physisorbed water molecules. The second weight loss occurs between 136–489°C, which is due to the decomposition of part of CS polymer and Chloramb

drug with 17.5% weight loss. The last weight loss occurs after 489°C with an 11% value.

After Chloramb incorporated with CS-IONPs, the total weight loss for Chloramb-CS-IONPs was increased higher than that of CS-IONPs. This evidence designated that the Chloramb drug was incorporated into CS-IONPs. The weight loss of Chloramb-CS-IONPs was 31.5%, while CS-IONPs has a 15.5%. So, Chloramb-CS-IONPs were evaluated to contain about 16.0 weight percentage of Chloramb. This content drug percentage was near to the value obtained from UV-vis spectroscopy with a 17.5 weight percentage.

Transmission Electron Microscopy

The transmission electron microscopy (TEM) technique was used to study the morphology of the nanoparticles. Figure 5A and B show the TEM images of the CS-IONPs and Chloramb-CS-IONPs, respectively. The CS-IONPs and Chloramb-CS-IONPs samples show a near-spherical shape and crystalline structure with an average diameter of about 15 nm.

Scanning Electron Microscopy

The Scanning Electron Microscopy (SEM) images were used to get more insight into the surface morphology of the nanoparticle samples. The CS-IONPs and Chloramb-

A CS-IONPs   **B Chloramb-CS-IONPs**
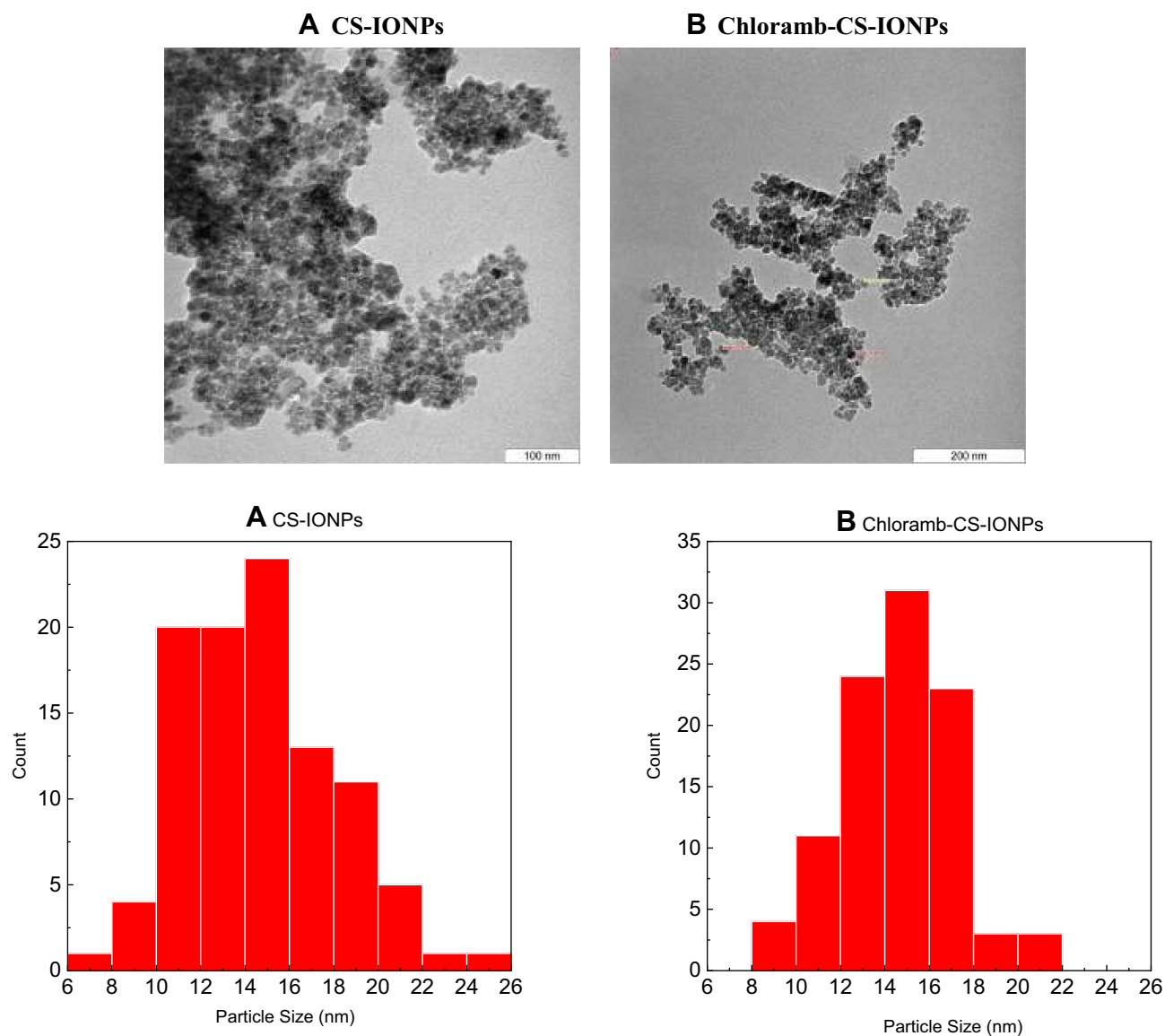
Figure 5 TEM image of CS-IONPs (**A**) and Chloramb-CS-IONPs (**B**).
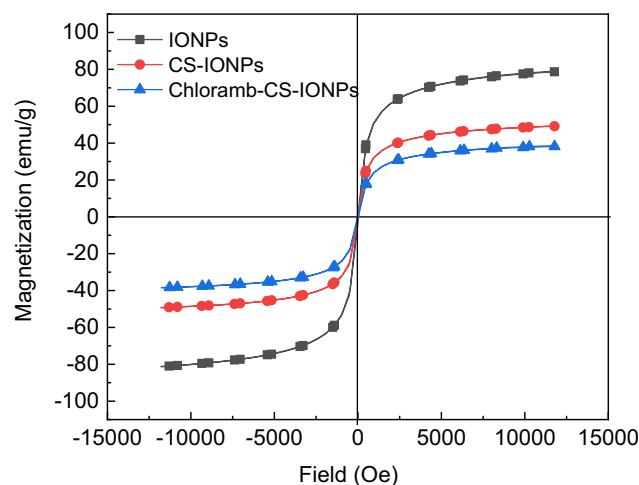
A CS-IONPs
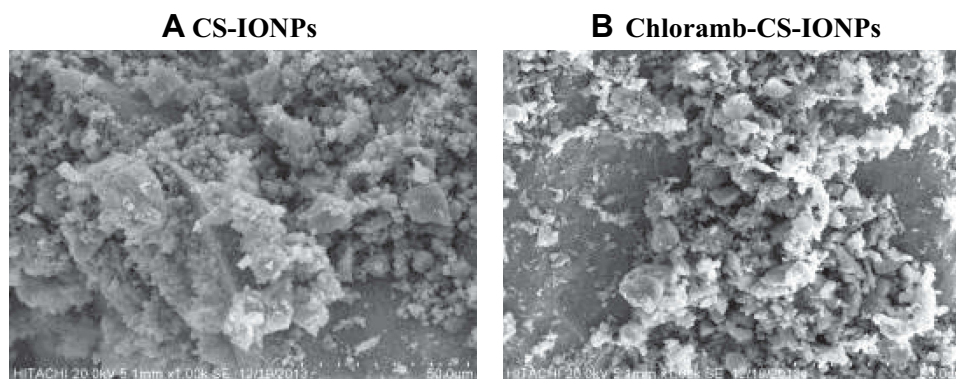
B Chloramb-CS-IONPs

Figure 6 Scanning Electron Microscopy (SEM) of CS-IONPs (**A**) and Chloramb-CS IONPs (**B**).

CS IONPs SEM images are shown in Figure 6A and B, respectively, where both of them represent flake-like morphology. The particles also show that they are agglomerated together which is due to drying the samples in an oven.

Measurement of Magnetic Properties

The magnetic properties of the IONPs nanoparticles with their drug-coated nanoparticles were evaluated using a vibrating sample magnetometer (VSM) at room temperature. The magnetic hysteresis curves of IONPs, CS-IONPs and Chloramb-CS-IONPs are shown in Figure 7. It appears from the figure that the magnetic saturation (Ms) for IONPs, CS-IONPs and Chloramb-CS-IONPs are 79.0, 49.1 and 38.6, respectively. All the magnetic hysteresis curves of the prepared samples have superparamagnetic

Figure 7 Magnetization curves of IONPs, CS-IONPs, and chloramb-CS-IONPs recorded at room temperature.

behavior. It can be seen from Figure 7 that the Ms of Chloramb-CS-IONPs and CS-IONPs was less compared to IONPs. The decrease in Ms value is only due to the exchange of electrons between the surface of Fe atoms with the CS.[42]

Loading and Release Behavior of Chlorambucil

The percentages of loading of Chloramb in Chloramb-CS-IONPs nanocomposite were calculated by ultraviolet-visible absorption spectroscopy. The loading percentage of Chloramb in the Chloramb-CS-IONPs nanocomposite was found to be around 19%. The release profiles of Chloramb from the Chloramb-CS-IONPs nanocomposite were investigated in phosphate-buffered solutions at pH 7.4 (Figure 8), showing that the maximum percentage release reaches about 89.9% within about 5000 min (83.3 h) at pH 7.4. The inset of Figure 8 shows the physical mixture of Chloramb and CS-IONPs exposed to the buffer solution at pH 7.4. It was found that Chloramb was quickly released from its physical mixture of CS-IONPs and the release was completed within 10 hours at pH 7.4. This physical mixture does not show any sustained-release effect; this is due to the low electrostatic attraction between the Chloramb and CS-IONPs.

Release Kinetics of Chloramb from the Chloramb-CS-IONPs Nanocomposite

Different kinetics models such as the zeroth-order,[43] pseudo-first-order, pseudo-second-order,[44] Higuchi model, Hixson model and Korsmeyer-Peppas[45] equations were used to investigate the release kinetics
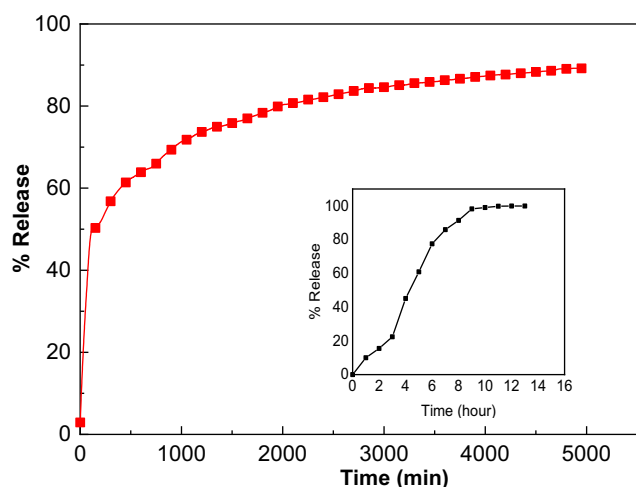
Figure 8 Release profiles of Chloramb from the Chloramb-CS-IONPs nanocomposite into phosphate buffered solution at pH 7.4.
Note: Inset shows the release profiles of Chloramb from its physical mixture of Chloramb and CS-IONPs at pH 7.4.

behavior of Chloramb from its Chloramb-CS-IONPs nanocomposite (Figure 9). Using these equations and models, it was found that the pseudo-second-order kinetic model can be better fitted to describe the release behavior of Chloramb from its Chloramb-CS-IONPs nanocomposite (Figure 9C) compared to the other models used in this study.
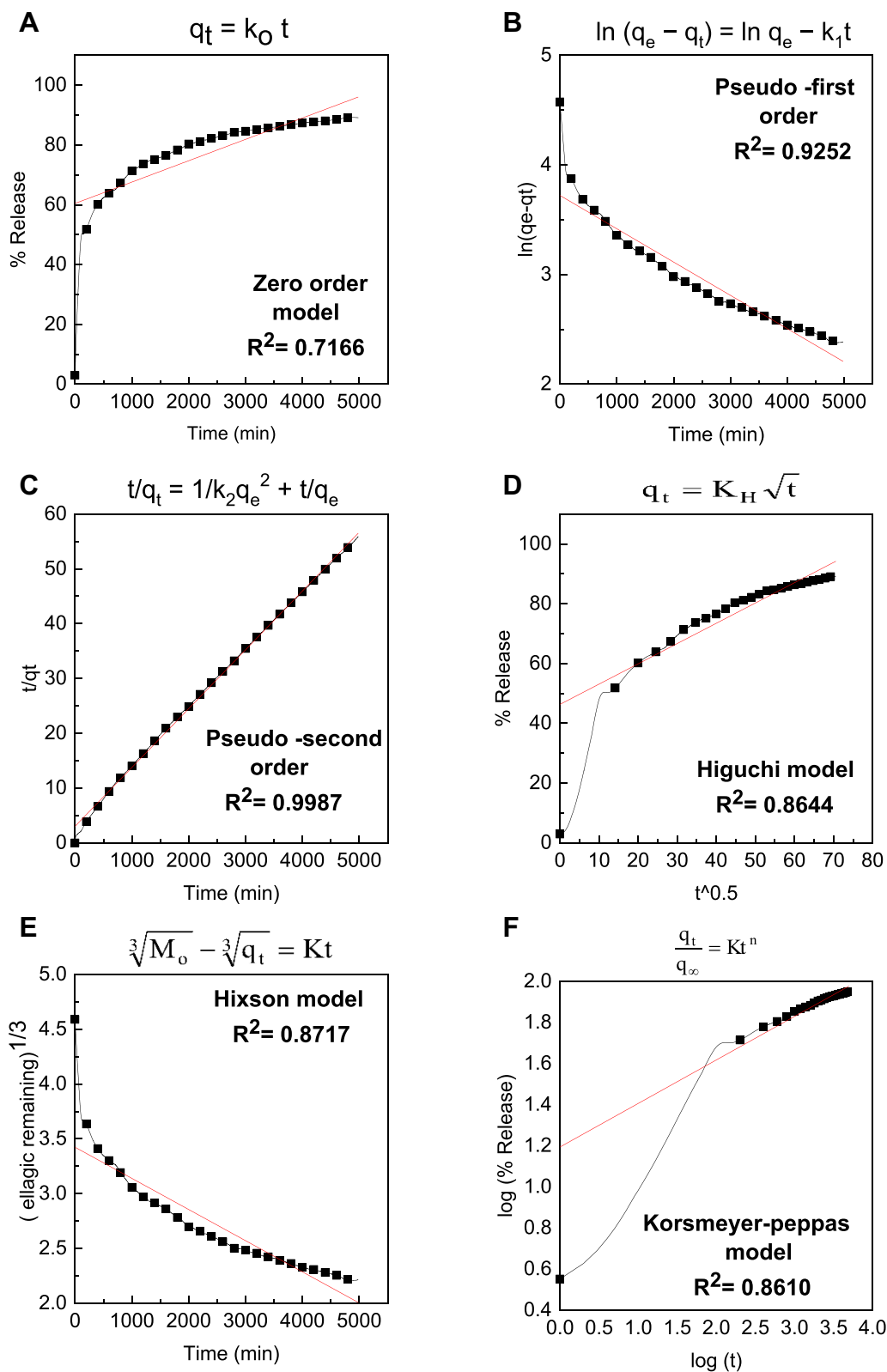
In vitro Bioassay

The cytotoxicity studies were estimated by treating the IONPs, CS-IONPs, Chloramb and Chloramb-CS-IONPs nanocomposite with normal fibroblast, 3T3 cells and cancer WEHI cells. The results were calculated as mean ± standard deviation for n = 3 independent experiments. Figure 10A and B shows the percentage cell viability of the 3T3 and WEHI cells, respectively, for all the samples. The IC_{50} of the Chloramb against normal fibroblast, 3T3 cell lines was found to be 35.47 μg/mL. It is noteworthy the IONPs, CS-IONPs, and Chloramb-CS-IONPs nanocomposite did not show any inhibitory action against the 3T3 cell lines. This result suggests that Chloramb-CS-IONPs nanocomposite is biocompatible with normal cells and would be very useful for use as a drug delivery system.

Based on Figure 10B and Table 1, the IC_{50} of the Chloramb and Chloramb-CS-IONPs nanocomposite

against WEHI cancer cells was found to be 27.67 and 11.12 μg/mL, respectively. The drug loading in the nanocomposite was calculated based on the ultraviolet-visible absorption spectroscopy and was found to be 19%. This result indicates that the $IC_{50} = 11.12$ for Chloramb-CS-IONPs nanocomposite contains 2.1 μg of the drug. If we compare the 2.1 μg of the drug in nanocomposite with IC_{50} of free Chloramb (27.67 μg/mL), this indicates that the anti-cancer properties of the drug were enhanced by 13 folds. This suggests that the designed Chloramb-CS-IONPs nanocomposite is very useful for targeting cancer cells without damaging/harming normal tissues.

Conclusion

The present study demonstrated better efficacy of IONPs loaded with Chloramb compared to its bare counterpart on the viability reduction of WEHI cancer cells. The anti-leukemia agent, Chlorambucil was loaded into CS-IONPs nanoparticles by the ionic gelation method to form Chloramb-CS-IONPs. The IONPs were stabilized using the CS polymer. Their nano-size regime and crystallinity were confirmed by TEM and XRD analysis, respectively. Both CS-IONPs nanoparticles and Chloramb-CS-IONPs nanocomposite have an average size of 15 nm. The loading efficiency of Chloramb in the Chloramb-CS-IONPs was estimated to be about 19% where the conjugation of IONPs with the drug was evidenced by the FTIR spectroscopy. The prepared CS-IONPs nanoparticles have a superparamagnetic property, and this property was retained in its Chloramb-CS-IONPs. The release profiles of Chloramb from its nanocomposite showed a controlled release property with 89.9% release within about 5000 min (83.3 h) and the release governs by the pseudo-second-order kinetic model. In this regard, the encapsulation of Chloramb within CS-IONPs nanoparticle brought a new avenue to improve the bioavailability properties of Chloramb and can make the drug-responsive for the treatment of cancer compared to its counterpart, free Chloramb. The IC_{50} of the Chloramb and Chloramb-CS-IONPs nanocomposite against WEHI cancer cells was found to be 27.67 and 11.12 μg/mL, respectively, with good biocompatible on 3T3 normal cell lines.

A

$$q_t = k_O t$$

Zero order model
$R^2 = 0.7166$

B

$$\ln(q_e - q_t) = \ln q_e - k_1 t$$

Pseudo -first order
$R^2 = 0.9252$

C

$$t/q_t = 1/k_2 q_e^2 + t/q_e$$

Pseudo -second order
$R^2 = 0.9987$

D

$$q_t = K_H \sqrt{t}$$

Higuchi model
$R^2 = 0.8644$

E

$$\sqrt[3]{M_o} - \sqrt[3]{q_t} = Kt$$

Hixson model
$R^2 = 0.8717$

F

$$\frac{q_t}{q_\infty} = Kt^n$$

Korsmeyer-peppas model
$R^2 = 0.8610$

Figure 9 Fitting the data of Chloramb release from Chloramb-CS-IONPs nanocomposite into different kinetics models (**A–F**).
Notes: The q_t is the release rate at time$t$; qe is the equilibrium release rate; k is a constant corresponding to release amount; Mt are the drug content remaining in nanocomposites at release times t; M0 is the drug content remaining in nanocomposite at release times 0.

A

B
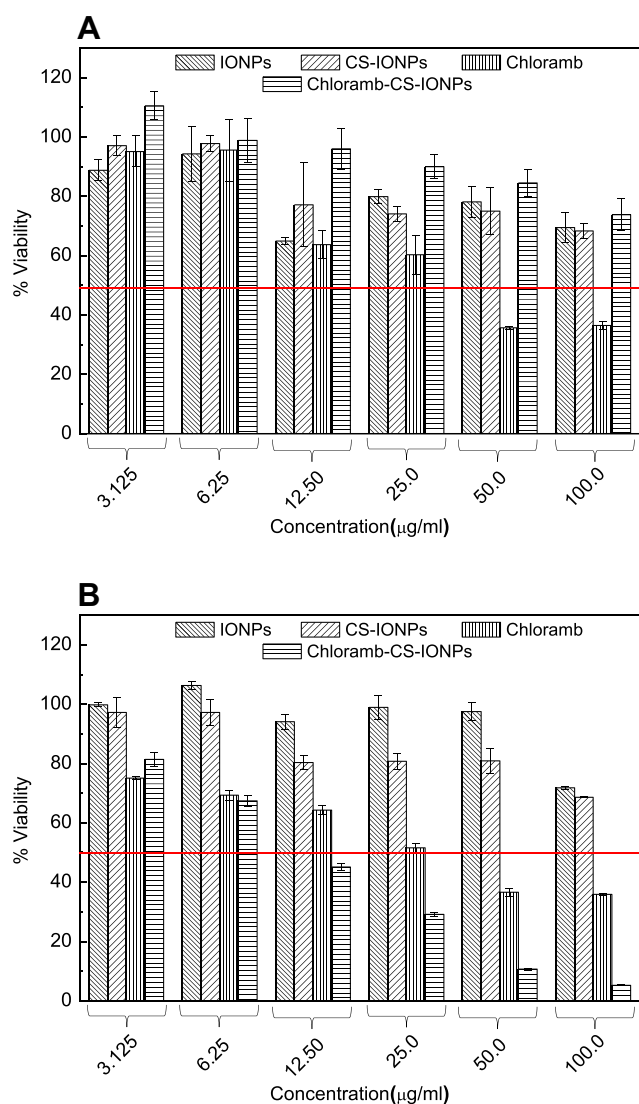
Figure 10 Cytotoxicity assay IONPs, CS-IONPs, Chloramb and Chloramb-CS-IONPs nanocomposite against normal fibroblast, 3T3 cells (**A**) and cancer WEHI cells (**B**).

Acknowledgment

Dr. Samer Al-Ali is thankful to the Isra University, Faculty of Pharmacy and Faculty of Science for providing the necessary facilities to carry out this research work. The

Table 1 The IC_{50} Value for IONPs, CS-IONPs, Chloramb and Chloramb-CS-IONPs Nanocomposite Tested on 3T3 and WEHL Cell Lines

	IC_{50} (µg/mL)	
	3T3	**WEHI**
IONPs	Non-toxic	Non-toxic
CS-IONPs	Non-toxic	Non-toxic
Chloramb	35.47	27.67
Chloramb-CS-IONPs	Non-toxic	11.12

Disclosure

The authors report no conflicts of interest in this work.

References

1. Siegel RL, Miller KD, Jemal A. Cancer statistics, 2016. *CA Cancer J Clin*. 2016;66(1):7–30.
2. Greaves M. Leukaemia'firsts' in cancer research and treatment. *Nat Rev Cancer*. 2016;16(3):163. doi:10.1038/nrc.2016.3
3. Jabbour E, Kantarjian H. Chronic myeloid leukemia: 2014 update on diagnosis, monitoring and management. *Am J Hematol*. 2014;89 (5):547–556. doi:10.1002/ajh.23691
4. Wierda WG, Byrd JC, Abramson JS, et al. NCCN guidelines insights: chronic lymphocytic leukemia/small lymphocytic lymphoma, version 2.2019. *Nat Comprehensive Cancer Network*. 2019;17(1):12–20. doi:10.6004/jnccn.2019.0002
5. Baudino A. Targeted cancer therapy: the next generation of cancer treatment. *Current Drug Discovery Technol*. 2015;12(1):3–20.
6. Prabhu RH, Patravale VB. Polymeric nanoparticles for targeted treatment in oncology: current insights. *Int J Nanomed*. 2015;10:1001.
7. Singh SK, Singh S, Lillard Jr JW, Singh R, et al. Drug delivery approaches for breast cancer. *Int J Nanomed*. 2017;12:6205.
8. Shenoy DB. Poly (ethylene oxide)-modified poly (-caprolactone) nanoparticles for targeted delivery of tamoxifen in breast cancer. *Int J Pharm*. 2005;293(1–2):261–270.
9. Jadon RS, Sharma M. Docetaxel-loaded lipid-polymer hybrid nanoparticles for breast cancer therapeutics. *J Drug Deliv Sci Technol*. 2019;51:475–484. doi:10.1016/j.jddst.2019.03.039
10. Du M, Ouyang Y, Meng F, et al. Polymer-lipid hybrid nanoparticles: a novel drug delivery system for enhancing the activity of Psoralen against breast cancer. *Int J Pharm*. 2019;561:274–282. doi:10.1016/j.ijpharm.2019.03.006
11. Zhou Z, Kennell C, Jafari M, et al. Sequential delivery of erlotinib and doxorubicin for enhanced triple negative breast cancer treatment using polymeric nanoparticle. *Int J Pharm*. 2017;530(1–2):300–307.
12. Almurshedi AS, Aljunaidel HA, Alquadeib B, et al. Development of inhalable nanostructured lipid carriers for ciprofloxacin for noncystic fibrosis bronchiectasis treatment. *Int J Nanomed*. 2021;16:2405.
13. Hussein-Al-Ali SH, Arulselvan P, Fakurazi S, et al. The in vitro therapeutic activity of betulinic acid nanocomposite on breast cancer cells (MCF-7) and normal fibroblast cell (3T3). *J Mater Sci*. 2014;49 (23):8171–8182.
14. Zohreh N, Hosseini SH, Pourjavadi A. Hydrazine-modified starch coated magnetic nanoparticles as an effective pH-responsive nanocarrier for doxorubicin delivery. *J Industrial Eng Chem*. 2016;39:203–209.
15. He L, Zheng R, Min J, et al. Preparation of magnetic microgels based on dextran for stimuli-responsive release of doxorubicin. *J Magnetism Magnetic Mater*. 2021;517:167394.
16. Ye Z, Zhang Y, Liu Y, et al. EGFR targeted cetuximab-valine-citrulline (vc)-doxorubicin immunoconjugates-loaded bovine serum albumin (BSA) nanoparticles for colorectal tumor therapy. *Int J Nanomed*. 2021;16:2443.
17. Mangaiyarkarasi R, Chinnathambi S, Karthikeyan S, et al. Paclitaxel conjugated Fe3O4@ LaF3: ce3+, Tb3+ nanoparticles as bifunctional targeting carriers for cancer theranostics application. *J Magnetism Magnetic Mater*. 2016;399:207–215.
18. Khodadadi E, Mahjoub S, Arabi MS, et al. Fabrication and evaluation of aptamer-conjugated paclitaxel-loaded magnetic nanoparticles for targeted therapy on breast cancer cells. *Mol Biol Rep*. 2021;48:1–12.

19. Gui G, Fan Z, Ning Y, et al. Optimization, characterization and in vivo evaluation of paclitaxel-loaded folate-conjugated superparamagnetic iron oxide nanoparticles. *Int J Nanomed*. 2021;16:2283.

20. Morovati A, Ahmadian S, Jafary H. Cytotoxic effects and apoptosis induction of cisplatin-loaded iron oxide nanoparticles modified with chitosan in human breast cancer cells. *Mol Biol Rep*. 2019;46 (5):5033–5039.

21. Bejjanki NK, Xu H, Xie M. GSH triggered intracellular aggregated-cisplatin-loaded iron oxide nanoparticles for overcoming cisplatin resistance in nasopharyngeal carcinoma. *Journal of Biomaterials Applications*. 2021;36(1):45–54. doi:10.1177/0885328220982151

22. Nandi S, Treatment of pancreatic cancer using gemcitabine-loaded superparamagnetic iron oxide nanoparticles (SPIONs). University of Liverpool; 2020.

23. Deda DK, Cardoso RM, Kawassaki RK, et al. Cytotoxicity of methotrexate conjugated to glycerol phosphate modified superparamagnetic iron oxide nanoparticles. *J Nanosci Nanotechnol*. 2021;21 (3):1451–1461. doi:10.1166/jnn.2021.19027

24. Nagesh PKB, Johnson NR, Boya VKN, et al. PSMA targeted docetaxel-loaded superparamagnetic iron oxide nanoparticles for prostate cancer. *Colloids Surf B Biointerfaces*. 2016;144:8–20. doi:10.1016/j.colsurfb.2016.03.071

25. Dou J, Li L, Guo M, et al. Iron oxide nanoparticles combined with cytosine arabinoside show anti-leukemia stem cell effects on acute myeloid leukemia by regulating reactive oxygen species. *Int J Nanomed*. 2021;16:1231.

26. Trujillo-Alonso V, Pratt EC, Zong H, et al. FDA-approved ferumoxytol displays anti-leukaemia efficacy against cells with low ferroportin levels. *Nature Nanotechnol*. 2019;14(6):616–622.

27. Kumar S, Dilbaghi N, Saharan R, Bhanjana G. Nanotechnology as emerging tool for enhancing solubility of poorly water-soluble drugs. *Bionanosci*. 2012;2(4):227–250.

28. Sareen S, Mathew G. Improvement in solubility of poor water-soluble drugs by solid dispersion. *Int J Pharm Investigation*. 2012;2(1):12.

29. Panasci L, Paiement JP, Christodoulopoulos G, et al. Chlorambucil drug resistance in chronic lymphocytic leukemia: the emerging role of DNA repair. *Clin Cancer Res*. 2001;7(3):454–461.

30. Reux B, Weber V, Galmier M-J, et al. Synthesis and cytotoxic properties of new fluorodeoxyglucose-coupled Chlorambucil derivatives. *Bioorg Med Chem Lett*. 2008;16(9):5004–5020. doi:10.1016/j.bmc.2008.03.038

31. Yordanov GG, Bedzhova ZA, Dushkin CD, et al. Preparation and physicochemical characterization of novel chlorambucil-loaded nanoparticles of poly(butylcyanoacrylate). *Colloid Polym Sci*. 2010;288 (8):893–899. doi:10.1007/s00396-010-2219-5

32. Assadi A, Assadi A, Sharifi Najafabadi V, et al. Novel Chlorambucil-conjugated anionic linear-globular PEG-based second-generation dendrimer: in vitro/in vivo improved anticancer activity. *Onco Targets Ther*. 2016;9:5531. doi:10.2147/OTT.S103487

33. Capolla S, Mezzaroba N, Zorzet S, et al. A new approach for the treatment of CLL using Chlorambucil/hydroxychloroquine-loaded anti-CD20 nanoparticles. *Nano Res*. 2016;9(2):537–548. doi:10.1007/s12274-015-0935-3

34. Akbarian S, Sojoodi J, Monnavari F, et al. Nano conjugated PLGA-chlorambucil: synthesis in vitro anti non-hodgkin's lymphoma cellular assay. *Lett Drug Des Discov*. 2017;14(7):827–836. doi:10.2174/1570180814666161130113446

35. Hussein-Al-Ali MZ, Al Ali S, Geilich B, et al. Synthesis, characterization, and antimicrobial activity of an ampicillin-conjugated magnetic nanoantibiotic for medical applications. *Int J Nanomed*. 2014;9:3801–3814. doi:10.2147/IJN.S61143

36. Hussein-Al-Ali SH, Arulselvan P, Fakurazi S, et al. The in vitro therapeutic activity of betulinic acid nanocomposite on breast cancer cells (MCF-7) and normal fibroblast cell (3T3). *J Mater Sci*. 2014;49 (23):8171–8182. doi:10.1007/s10853-014-8526-3

37. Andrade ÂL, Souza DM, Pereira MC, et al. pH effect on the synthesis of magnetite nanoparticles by the chemical reduction-precipitation method. *Química Nova*. 2010;33(3):524–527.

38. Inbaraj BS, Tsai TY, Chen BH. Synthesis, characterization and antibacterial activity of superparamagnetic nanoparticles modified with glycol chitosan. *Sci Technol Adv Mater*. 2012;13:015002.

39. Liu X, Hu Q, Fang Z, et al. Magnetic chitosan nanocomposites: a useful recyclable tool for heavy metal ion removal. *Langmuir*. 2009;25(1):3–8.

40. Hwang S, Umar A, Dar GN, et al. Synthesis and characterization of iron oxide nanoparticles for phenyl hydrazine sensor applications. *Sensor Letters*. 2014;12(1):97–101.

41. Zhang S, Zhang Y, Liu J, et al. Thiol modified Fe3O4@ SiO2 as a robust, high effective, and recycling magnetic sorbent for mercury removal. *Chem Eng J*. 2013;226:30–38.

42. Hussein-Al-Ali SH, El Zowalaty ME, Hussein MZ, et al. Novel kojic acid-polymer-based magnetic nanocomposites for medical applications. *Int J Nanomed*. 2014;9:351.

43. Akyuz LJM. An imine based COF as a smart carrier for targeted drug delivery: from synthesis to computational studies. *Microporous Mesoporous Mater*. 2020;294:109850.

44. Oladipo AO, Nkambule TT, Mamba BB, Msagati TA. The stimuli-responsive properties of doxorubicin adsorbed onto bimetallic Au@ Pd nanodendrites and its potential application as drug delivery platform. *Mater Sci Eng C*. 2020;110:110696.

45. Dathathri E, Lal S, Mittal M, et al. Fabrication of low-cost composite polymer-based micro needle patch for transdermal drug delivery. *Appl Nanosci*. 2020;10(2):371–377.